FLUIDICS

S-69-1089

FINAL REPORT

DESIGN, DEVELOPMENT, FABRICATION AND DELIVERY OF FLUIDIC ACCELEROMETERS

Prepared for

George C. Marshall Space Flight Center
Astrionics Laboratory
NASA, Huntsville, Alabama

Contract No. NAS 8-20729

Prepared by

C. G. Ringwall
General Electric Company
Specialty Fluidics Operation
Schenectady, New York

May 23, 1969

SPECIALTY FLUIDICS OPERATION
GENERAL ELECTRIC
NEW BUSINESSES DEVELOPMENT OPERATION
SCHENECTADY, NEW YORK

FINAL REPORT

DESIGN, DEVELOPMENT, FABRICATION AND DELIVERY OF FLUIDIC ACCELEROMETERS

Prepared for:

George C. Marshall Space Flight Center
Astrionics Laboratory
NASA, Huntsville, Alabama

Contract No.:

NAS 8-20729

Prepared by:

C. G. Ringwall
General Electric Company
Specialty Fluidics Operation
Schenectady, New York

May 23, 1969

TABLE OF CONTENTS

LIST OF FIGURES

NOMENCLATURE

A	Nozzle area, in^2
G	Proportional gain, in.lb/rad
g	Damping amplifier gain, in.lb.sec.
H	Angular momentum, in.lb.sec.
I_s	Moment of inertia of rotor about spin axis, $in.lb.sec^2$
I	Moment of inertia of rotor about minor axis, $in.lb.sec^2$
k	Rotor damping coefficient, in.lb.sec.
ΔP	Differential pressure, psi
r	Moment arm, in.
R	Radius, in.
T	Torque about designated axis, in.lb.
t	Time constant, sec.
Θ	Angular displacement, rad

SECTION I - SUMMARY

Background

This report presents the result of work done on Contract NAS 8-20729. The contract was supported by the George C. Marshall Space Flight Center, Astrionics Laboratory, NASA, Huntsville, Alabama. Mr. C. S. Cornelius was the NASA Project Engineer.

The objective of the current program was to develop a method of producing a pressure signal proportional to angular rate. Several alternative approaches investigated the feasibility of integrating the output of an accelerometer developed in earlier phases of the program. The accelerometer approach was also compared to a direct measurement of angular rate utilizing a gyro. On the basis of this comparison a two axis fluidic rate gyro was selected as the method to be further developed.

Analytical studies were performed to determine the optimum loop configuration, design layout and other parameters for the selected method. A breadboard test model of the gyro was constructed to demonstrate basic feasibility.

Technical Approach

Of the five approaches considered as potential angular rate sensors, two were concerned with integrating the output of an accelerometer developed earlier in the program. The remaining three implementations involved a direct measurement of angular rate.

Integration of the accelerometer output to obtain angular rate was rejected because of the complex mechanization and limited system application.

The chosen two axis gyro approach was compared to a two axis gyro utilizing a liquid filled rotor and also to a gimballed single degree of freedom gyro. Selection of the developed approach was based on the inherent simplicity of the mechanical structure, its temperature and supply pressure insensitivity and its compatibility with a broad range of control applications.

The selected approach utilizes fluidic pickoffs and amplifiers to sense the angular displacement of a rotor (relative to the gyro housing) in two control axes. The resulting error signals are further utilized to slave the rotor spin axis to the housing. The differential pressure across the torquing jets is directly related to input rate on the corresponding sensitive axis of the gyro. This approach has the obvious advantage of combining the functions of two single degree of freedom gyros in one unit consisting of a single rotor and air bearing.

Major design goals achieved in the program were both the development of a stable air bearing configuration as well as demonstration of the feasibility of closing fluidic damping and torquing loops around the gyro rotor.

Functional Description of Two Axis Gyro

The rotor and hydrostatic air bearing configuration selected for the feasibility model is shown in Figure 1. The rotor is a sphere with a flange on the equatorial plane of the rotor and is supported in a hydrostatic bearing consisting of two hemispherical end caps. Figure 2 shows the functional blocks required to close the loops around the gyro rotor. An angle pickoff and two control loops are required for each axis. Operation of the gyro is as follows:

Assume an angular rate is applied about the y axis. In the absence of externally applied torques the rotor spin axis remains fixed relative to space. The result is an angular displacement between the gyro case and the rotor flange (about the y axis). This displacement is sensed by a pneumatic sensor physically located on the x axis, the error signal is amplified and applied to a pair of differential torquing nozzles located on the y axis. The resulting torque applied about the x axis causes the gyro rotor to precess about the y axis in a direction to null the angular displacement. The closed loop mode forces the steady state precession of the rotor about the y axis to be equal to the angular velocity of the case about the y axis. The torque required to maintain the rotor slaved to the case is equal to the angular momentum of the gyro rotor multiplied by the angular rate of the gyro housing about the y axis. This torque is directly related to the pressure differential across the torquing nozzles. The pressure differential is the gyro output. The scale factor is a direct function of the angular momentum and an inverse function of the area of the torquing nozzles and the torquing nozzle moment arm.

The angle pickoff located on the y axis is sensitive to angular displacements about the x axis. The output of this pickoff is amplified and torques the rotor in a direction to slave the rotor to the case (for rotation about the x axis). With both loops closed, the rotor spin axis is slaved to a case axis passing through the poles of the bearing caps. The differential pressures across the two sets of torquing nozzles are proportional to angular rates about the corresponding sensitive axis of the gyro.

The damping amplifiers shown in Figure 2 are used to stabilize the closed loop. The transfer function for the primary torquing loop has a pole with negligible damping occurring at the rotor nutation frequency. Without the damping amplifier the primary torquing loop would oscillate at the nutation frequency which is 1.7 times the rotor spin frequency for the gyro configuration shown in Figure 1. The damping loop consists of a derivative network and a set of torquing nozzles. The loop output is applied as a torque about the same axis as the angular displacement occurs and adds sufficient damping to insure less than unity loop gain at the gyro nutation frequency.

The closed loop bandwidth of the gyro is determined by the open loop crossover of the primary torquing loop. The crossover frequency is directly proportional to the gain (torque/radian) and inversely proportional to the angular momentum of the rotor. With adequate nutation damping the bandwidth can approach the nutation frequency of the gyro rotor.

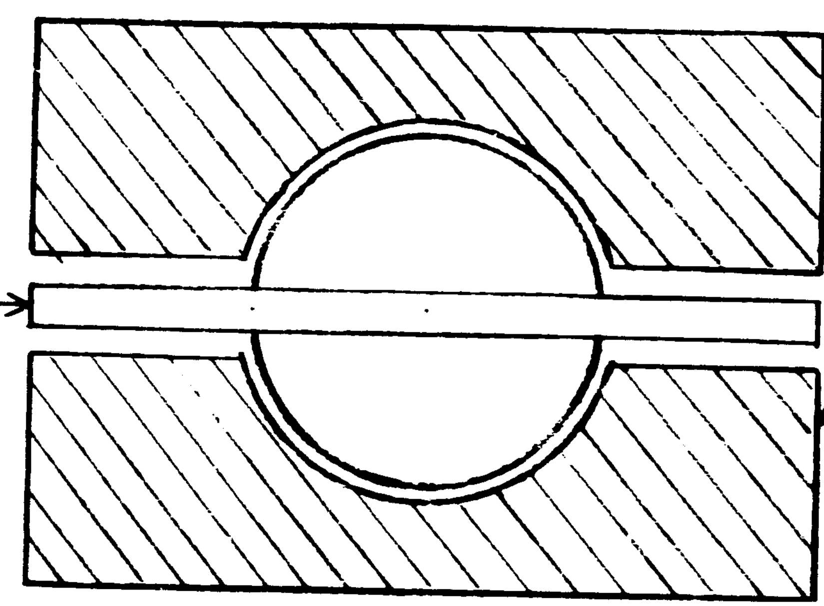

Figure 1. Air Bearing and Rotor Schematic

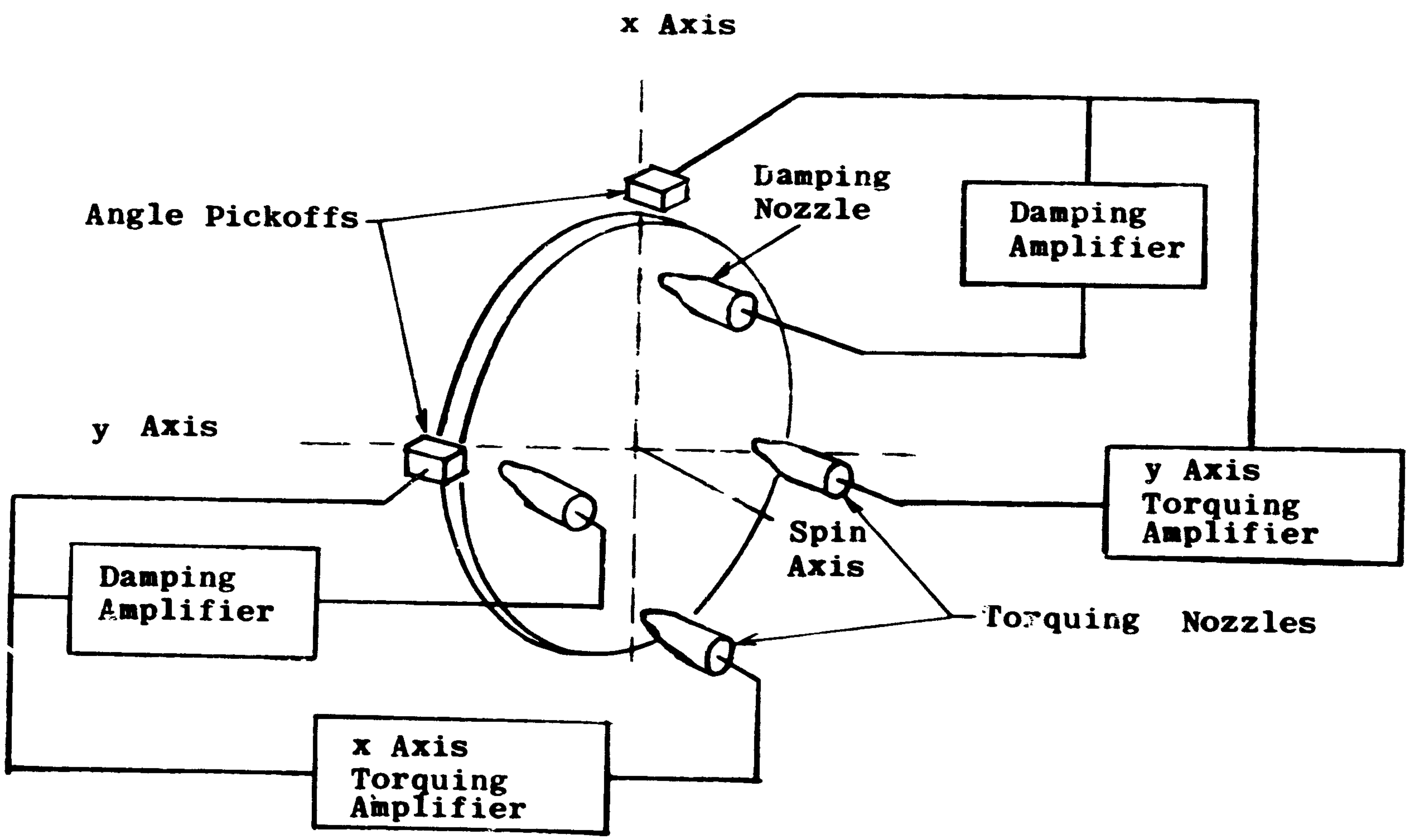

Figure 2. Gyro Schematic

Hardware Description

The circuit diagram for one channel of the gyro is shown in Figure 3 The angle pickoff is a bridge circuit consisting of two variable and two fixed resistors The variable resistors are two .02 inch diameter orifices directed at the edges of the rotor flange. Displacement of the rotor flange relative to the orifices increases the resistance of one orifice while decreasing the resistance of the other. The resulting differential pressure signal is applied to the control ports of amplifier number 1 The signal is amplified by amplifiers 1 and 2; the output of number 2 drives both the primary torquing amplifier (3) and the damping amplifiers (4 and 5). Both the supply pressure and aspect ratios of the amplifiers have been selected to satisfy the overall gain and maximum torquing requirements.

Amplifier number 5 in the damping channel performs the derivative function The output of this amplifier is shunted to local ambient by a fluidic inductor. This particular configuration was chosen because it essentially eliminates steady state flow through the damping nozzles. Steady state gain or flow through the damping nozzles is a source of cross coupling between axis.

The fluidic circuit is packaged in a "stack-pack" format using laminated amplifiers and interconnecting laminates. Figure 4 shows the laminates, stack-up and circuit schematic for the three amplifier cascade in the primary torquing loop.

Figure 5 is a photograph of the gyro assembly. Figure 5(b) is an exploded view showing the rotor and the spherical bearing. The bearings are made as an integral part of two end plates which are aligned and then doweled to a common base plate. The torquing and damping nozzles are drilled into the inner face of the end plates; an air jet is directed against the face of the flange to torque the rotor Channels drilled in the end plate route the flow from the fluidic amplifiers to the appropriate torquing nozzles and also provide the gas flow to the bearing. The fluid amplifiers for one channel are assembled in two stacks and mounted on a common manifold. One channel is mounted on the top surfaces of the end plates while the second channel is mounted on the side surfaces. The angle pickoff orifices are drilled into the bottom surface of the amplifier manifold plate and connect directly to the control ports of the first stage. Shims are used between the amplifier manifold and the mounting surface to provide a nominal gap of .004 inches between the angle pickoff orifices and the rotor flange.

The rotor is fabricated from a precision ground 0.750 inch steel sphere; an aluminum flange is attached to the sphere by means of a shrink fit The flange is two inches in diameter by 0.100 inch thick. The torque required to spin the rotor is provided by spin jets directed tangentially to the end surfaces of the flange. Rotor caging is accomplished by contacting a nylon button on the spherical surface of the rotor. This button is inserted through the pole of one of the air bearings and produces a torque to precess the rotor spin axis under the button.

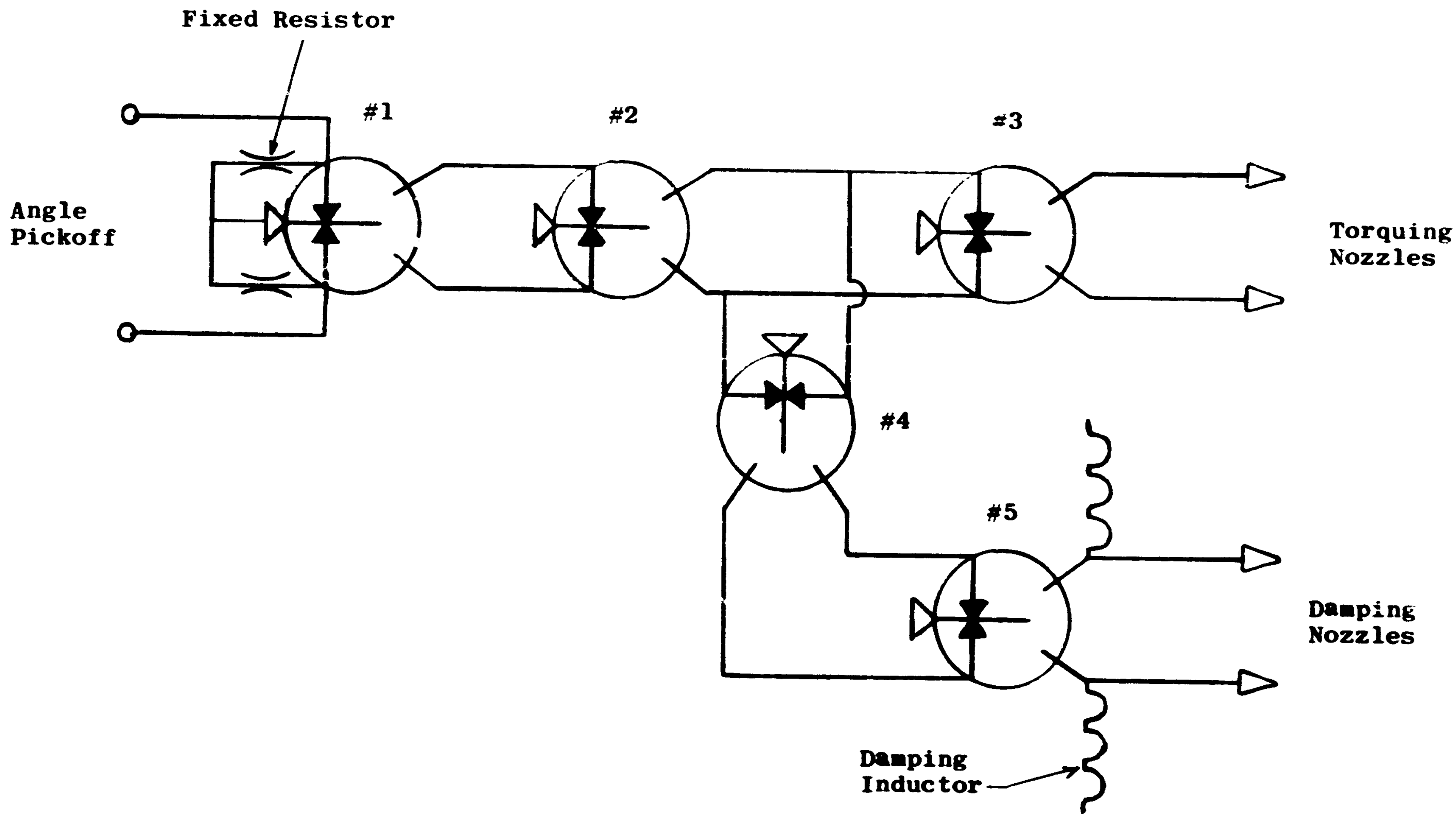

Figure 3. Circuit Diagram

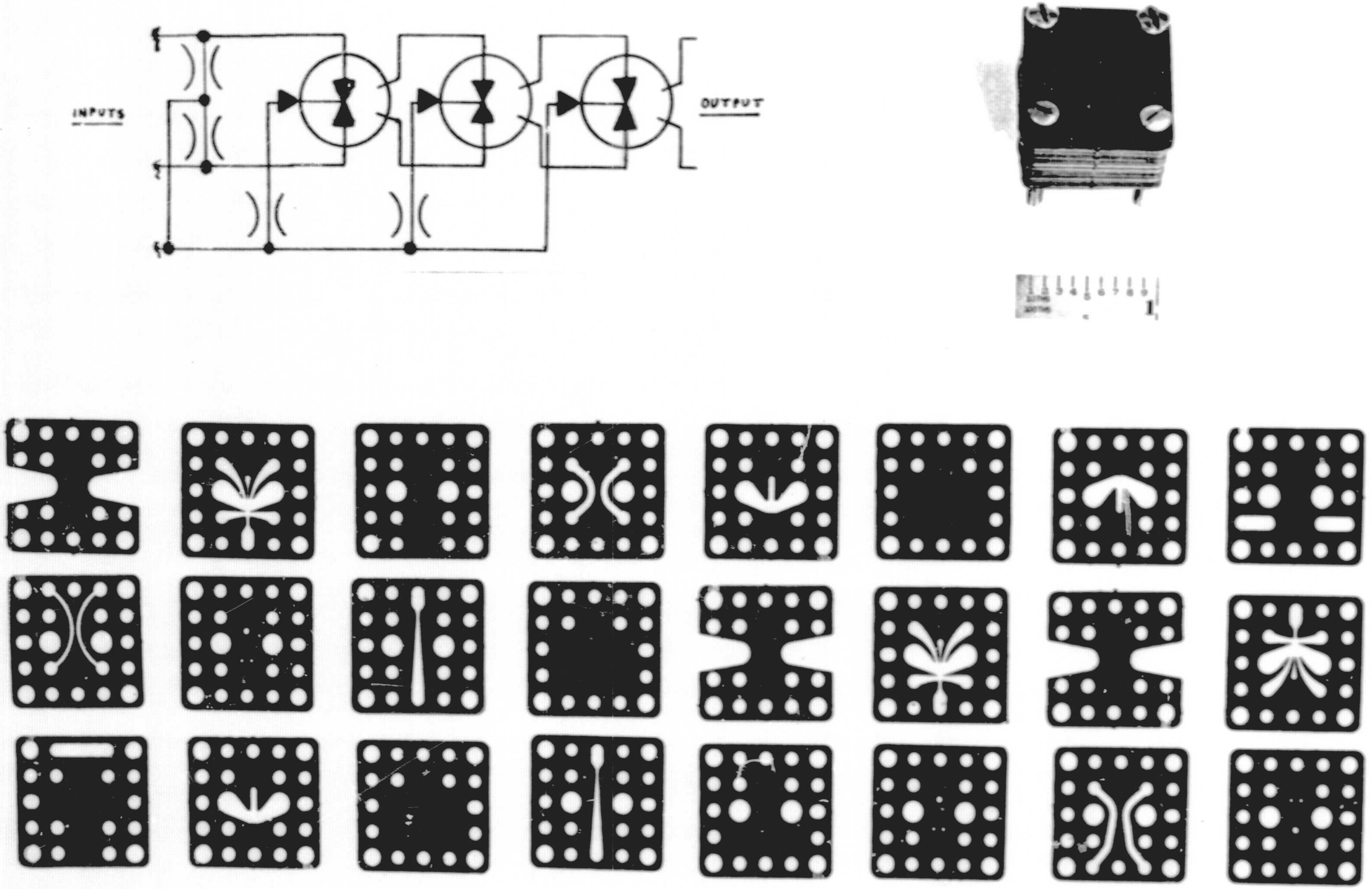

Figure 4. Three-amplifier Cascade Assembly Showing Laminates, Stack-up and Circuit Schematic

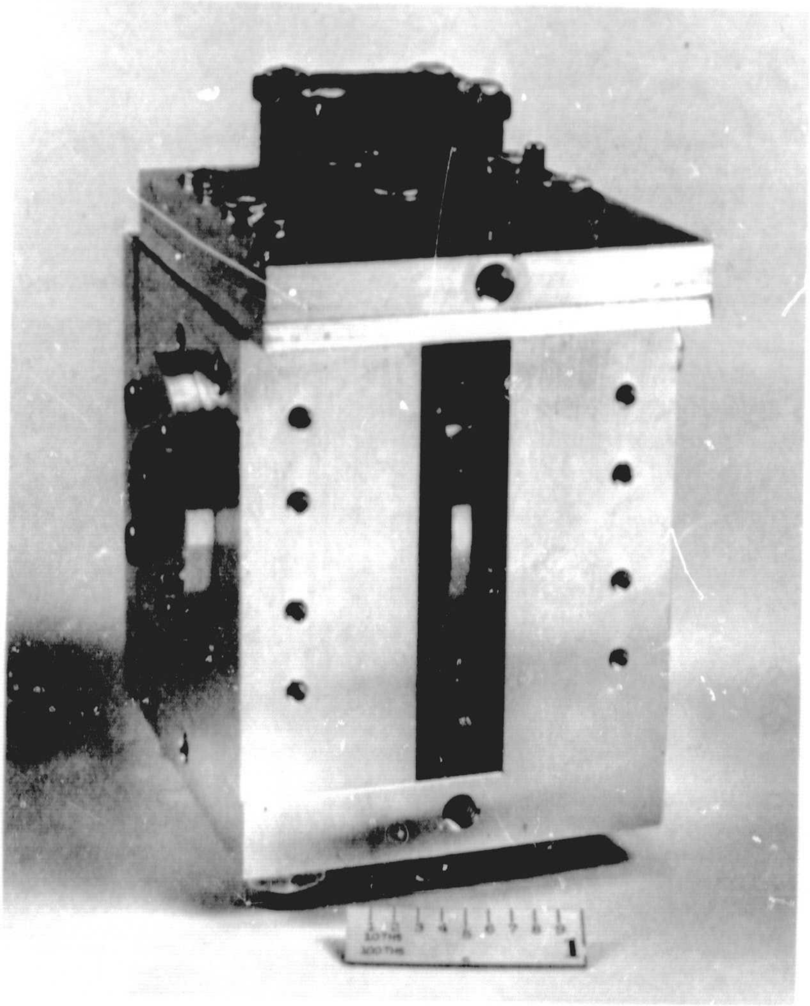

Figure 5a. Complete Rate Gyro Assembly

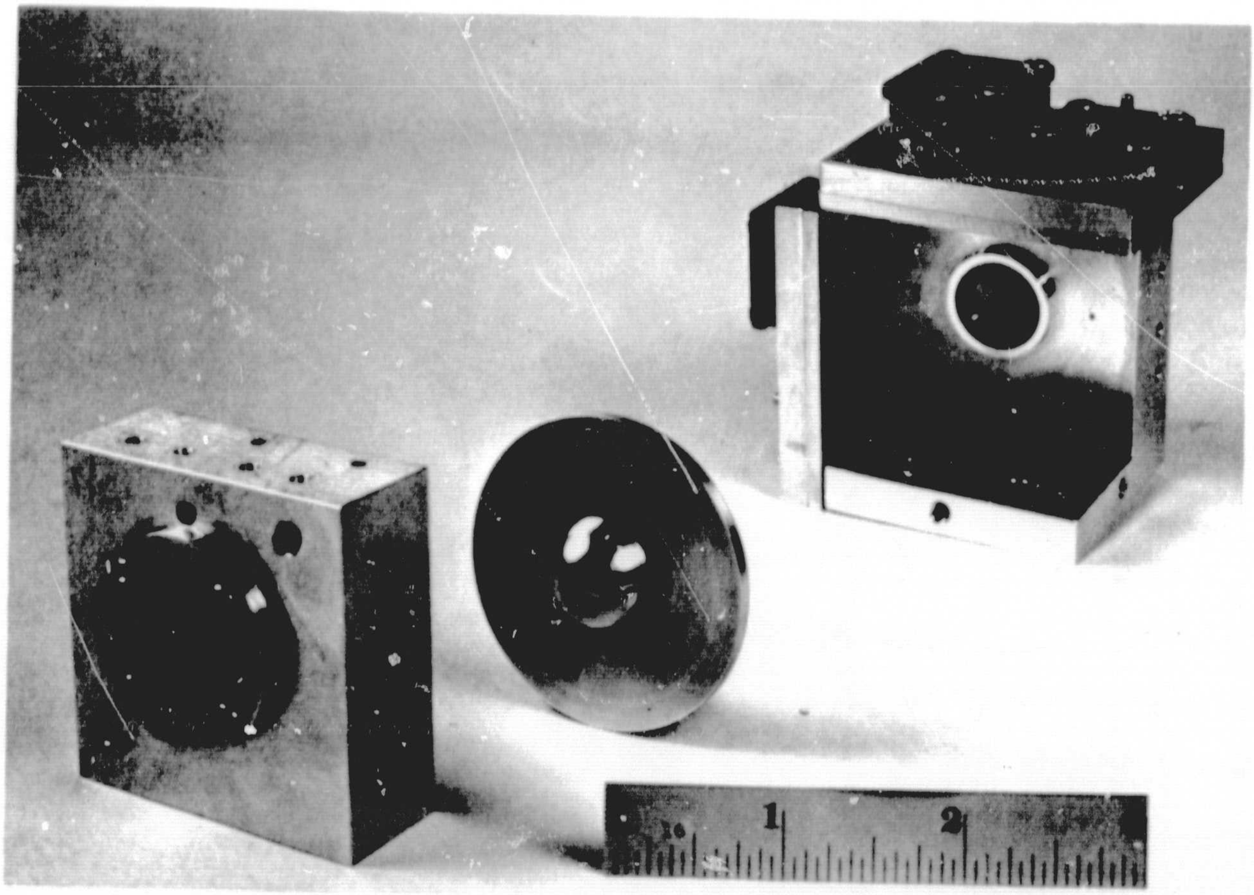

Figure 5b. Exploded View of Rate Gyro Assembly

Results

Stable operation of the air bearing and fluidic torquing loops was demonstrated with the feasibility hardware and a scale factor of .2 psi/deg/sec was measured. This scale factor is approximately fifty times that achievable with other fluidic gyro approaches (vortex gyro, etc). The design value scale factor was .4 psi/deg/sec; the lower experimental value is partly attributed to excessive torque gradients on the rotor. The gyro loops were operated with sufficient gain to give a 40 rad/sec gyro bandwidth while still retaining adequate nutation damping. The loops were operated stable over a rotor speed range of 3000 to 5000 RPM. The basic loop configuration and the circuit mechanization used on the feasibility model are satisfactory. The damping circuit however requires additional development to establish the optimum mechanization from the standpoint of packaging.

The torque gradients identified earlier also produced substantial cross coupling within the gyro and the major test effort on the breadboard gyro was directed at identifying those sources of torque coupling. The primary sources of torque were found to be:

1) Secondary flows induced by the rotor spin jets which produce torques on the rotor by coupling to the flat faces of the rotor flange.

2) Flow from the angle pickoff orifices which couple to the rotor flange and exert a centering torque on the rotor.

3) Gas flow through the bearing gap which produces a torque acting on the spherical rotor surface. Misalignment of the two bearing caps can also produce a bias torque and a torque gradient due to the geometry of the bearing and rotor.

The magnitude of torque coupling, in particular those associated with the secondary flows, is influenced by surfaces near the periphery of the rotor flange. The reduction of the torque coupling to the extent required to make an operational gyro requires a redesign of both the air bearing and rotor, as well as changes in the overall layout to remove amplifier manifolds and other supporting structures from the peripheral region of the rotor. The breadboard gyro assembly has been especially useful in identifying these sources of torque. Sufficient information was obtained to establish a gyro rotor and bearing configuration which will reduce the known sources of torque to acceptable values.

Design Recommendations

The recommended configuration is shown in Figure 6. The rotor is supported from the inside as contrasted to the outside support used on the feasibility model. The inside support circumvents critical bearing alignment procedures required on the feasibility model. The component parts requiring alignment are on the rotating rotor and torques resulting from misalignment are alternating torques with a frequency equal to the rotor spin frequency. On the feasibility configuration the direction of the misalignment torque

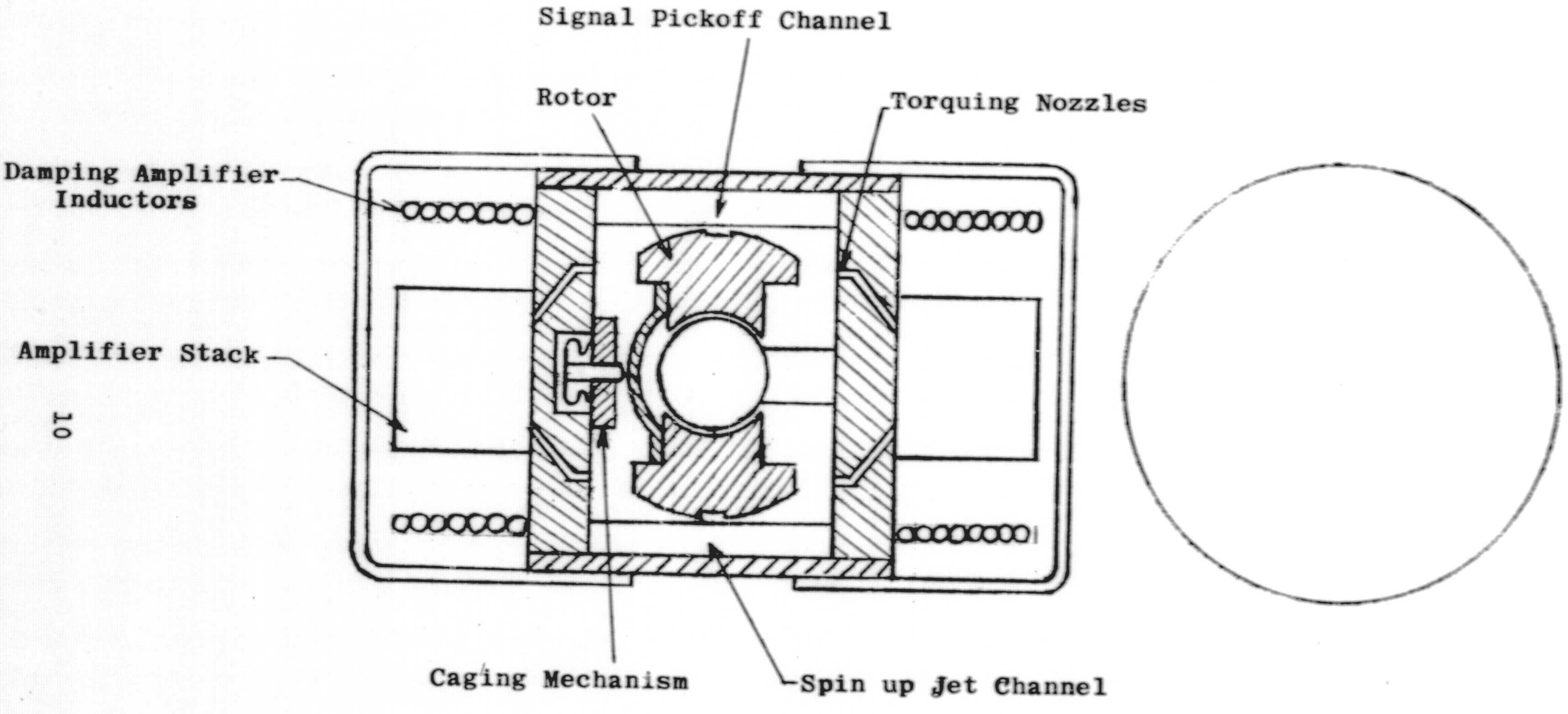

Figure 6. Recommended Design Layout

remained fixed relative to the rotor spin axis and produced a bias torque.

The outside of the rotor should be designed as a spherical surface with a shallow groove on the equatorial plane. The groove is used in conjunction with two sensing orifices to produce an angle read-out signal. The spherical surface extending out from the sides of the groove prevents torque coupling of the sensor flow to the rotor. This was a major source of coupling on the feasibility model. The rotor spin jets are directed tangentially to the surface and in a plane perpendicular to the spin axis. The spherical surface decouples the rotor from secondary flows induced by the spin jets since the pressures act normal to the spherical surface and thus will always pass through the center of support.

A caging cap is attached to one end of the rotor. To cage the rotor a pressure actuated nylon button is brought in contact with the caging cap forcing the rotor spin axis to align itself under the button.

The two fluidic amplifier stacks for the two channels are located at opposite ends of the rotor. All the torquing nozzles associated with one channel can be directed at one end of the rotor; hence, no crossover channels are required. This arrangement permits a relatively unimpeded and symmetrical vent region around the periphery of the rotor.

The estimated package size is a cylindrical envelope 2.5 inches in diameter by 3.5 inches long; the estimated weight is .7 lbs.

SECTION II - TECHNICAL DISCUSSION

Gyro Transfer Function

The open loop transfer function can be derived by summing torques about two axes on the rotor.

The two gyros designated x and y, lie in the plane of the rotor flange and are mutually perpendicular as shown in the following sketch.

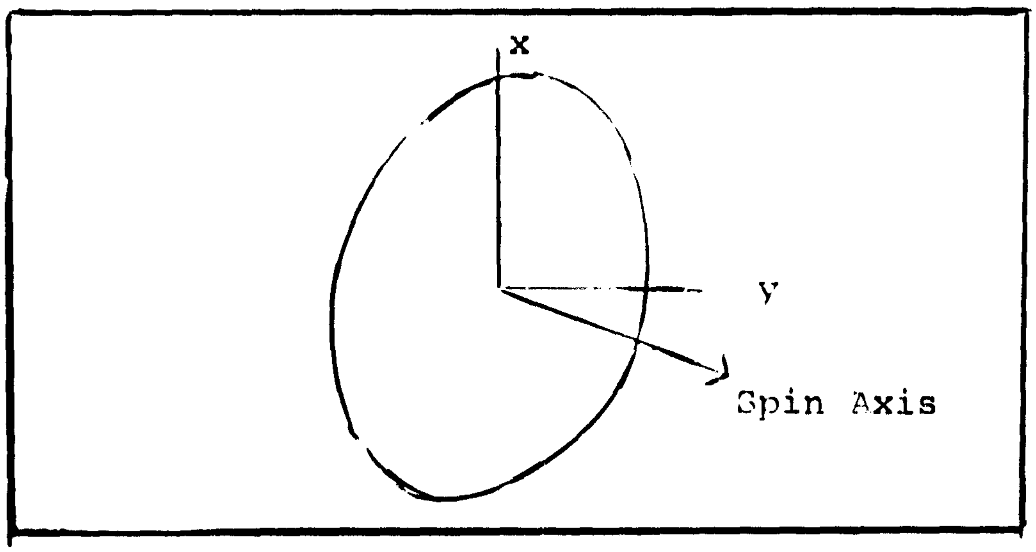

Assume the angular precession of the rotor about x and y is negligible compared to the gyro spin rate, then the summation of torques can be expressed by:

$$T_x = HS\Theta_y + IS^2\Theta_x + kS\Theta_x \quad (1)$$

$$T_y = -HS\Theta_x + IS^2\Theta_y + kS\Theta_y \quad (2)$$

where: H = angular momentum of rotor
I = momentum of inertia of rotor about either x or y
k = damping coefficient of rotor bearing
Θ = angular displacement about either x or y relative to an inertial reference
T = torque about the designated axis
S = Laplace operator.

To close a torquing loop around the rotor the angular displacement must be sensed around one axis and a torque applied about the other axis to cause the rotor to precess about the axis on which the angular displacement occurs.

Assume an amplifier with a gain (G) is used to generate the torques, then

$$T_x = -G\Theta_{\varepsilon y}$$

$$T_y = G\Theta_{\varepsilon x}$$

Θ_ε is the angular displacement error.

The sign associated with the gain is selected to produce the correct direction of precession to null the displacement error. Thus,

$$-G\Theta_{\varepsilon y} = HS\Theta_y + IS^2\Theta_x + kS\Theta_x \tag{3}$$

$$G\Theta_{\varepsilon x} = -SH\Theta_x + IS^2\Theta_y + kS\Theta_y \tag{4}$$

The open loop transfer function for the y channel can be derived from equations 3 and 4 by noting that in the x channel $\Theta_{\varepsilon x} = \Theta_x$.

$$\frac{\Theta_y}{\Theta_{\varepsilon y}} = \frac{G\ (G + HS)}{S[I^2S^3 + 2kIS^2 + (H^2+k^2)\ S + GH]} \tag{5}$$

For any practical gyro the angular momentum (H) will be much larger than the damping factor (k). Assuming that H>>k, equation 5 reduces to:

$$\frac{\Theta_y}{\Theta_{\varepsilon y}} = \frac{G}{HS\left[\frac{I^2S^2}{H^2} + \frac{2kIS}{H^2} + 1\right]} \tag{6}$$

The gyro rotor has equal moments of inertia about the y and x axis; hence, the transfer function for the x axis is identical to the y axis.

From equation 6 it is apparent that the transfer function has a pole at a frequency equal to H/I. The angular momentum is equal to the product of rotational velocity (ω_s) and the moment of inertia of the rotor about the spin axis (I_s).

Designating the frequency at which the pole occurs as ω_n, then:

$$\omega_n = \left(\frac{I_s}{I}\right)\omega_s$$

This is commonly referred to as the nutation frequency of the rotor. Generally, $I_s > I$; hence, the nutation frequency will be greater than the rotational frequency of the rotor.

Equation 6 can now be expressed by:

$$\frac{\Theta_Y}{\Theta_{\epsilon y}} = \frac{G}{HS\left[\frac{S^2}{\omega_n^2} + \frac{2k}{H}\frac{S}{\omega_n} + 1\right]} \qquad (7)$$

The closed loop transfer function can be derived directly from equation 7 and becomes:

$$\frac{S\Theta_Y}{S\Theta_{yi}} = \frac{G}{HS\left[\frac{S^2}{\omega_n^2} + \frac{2k}{H}\frac{S}{\omega_n} + 1\right]\left[1 + \frac{G}{HS\left(\frac{S^2}{\omega_n^2} + \frac{2k}{H}\frac{S}{\omega_n} + 1\right)}\right]} \qquad (8)$$

The gyro scale factor can be deduced directly from equation 8. The open loop transfer function has an integration; hence, for steady state input rates

$$\frac{S\Theta_Y}{S\Theta_{yi}} = 1.0$$

However, for steady state conditions the gyro precession ($S\Theta_Y$) is equal to the applied torque divided by the angular momentum. Assuming the applied torque is produced by a differential pressure across a pair of torquing nozzles

$$\frac{\Delta P}{S\Theta_{yi}} = \frac{H}{Ar} \qquad (9)$$

where: ΔP = the differential pressure and becomes the gyro output
Ar = product of nozzle area and moment arm

The scale factor is then a function of only the angular momentum and the geometry of the torquing nozzles.

Closed Loop Stability

The closed loop stability criteria can be deduced from the open loop transfer function for a single axis. Figure 7 is an amplitude vs frequency plot of the trnasfer function given by equation 7. The first crossover occurs on a -20 db per decade slope. If this crossover is made sufficiently low by reducing the gain of the torquing loop, the loop will be stable. The transfer function gain at ω_n must be below unity to satisfy stability requirements. The transfer function gain at ω_n is given by:

$$\frac{\theta_y}{\theta_\varepsilon} = \left| \frac{G}{2k\omega_n} \right| < 1.0 \tag{10}$$

The loop crossover (ω_c) is given by the ratio of gain (G) to angular momentum (H). The maximum loop crossover to satisfy stability is then given by:

$$\omega_c < \frac{2k\omega_n}{H} \tag{11}$$

The crossover frequency is approximately equal to the closed loop bandwidth of the gyro and as a result satisfying the stability criteria limits the maximum gyro bandwidth. Typically a bearing of the type used on the feasibility model will have a k of approximately 3 (10^{-7}) in.lb.sec. If the rotor is spun at 5000 RPM, ω_n will be 520 rad/sec and H will be .025 in.lb.sec. Substituting these values in equation 11, the maximum gyro bandwidth becomes approximately .01 rad/sec. Application requirements generally dictate gyro bandwidths on the order of 50 to 100 rad/sec and it becomes obvious that some type of signal shaping networks are required to get stable closed loop operation with useable bandwidth.

The following four basic approaches to stabilizing the loop were evaluated.

1. Lag compensation in the primary torquing loop.
2. Increasing the inherent damping of the rotor.
3. Parallel damping loops.
4. Lead compensation in the primary torquing loop.

Approach number 3 was selected for the feasibility gyro. The four approaches are described in the following sections.

Lag Compensation - It is apparent from the open loop transfer function, equation 7, that the first open loop crossover will have a phase margin of nearly 90°. This is considerably more phase margin than required. The addition of a lagging time constant occurring at the crossover frequency will decrease the phase margin to 45°. This is adequate for stability.

The open loop transfer function with a lag time constant occurring at the open loop crossover (ω_c) is given by:

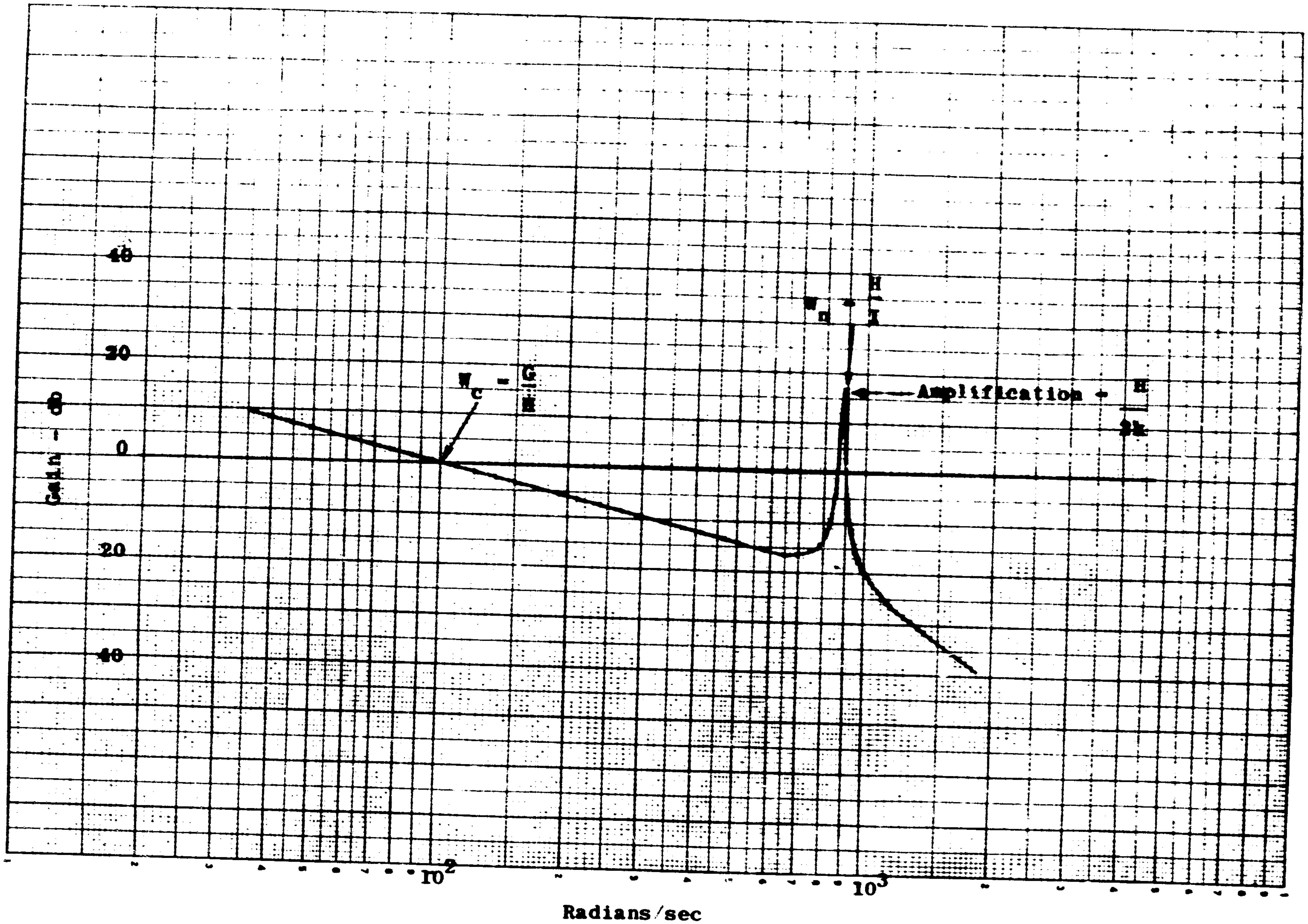

Figure 7. Gyro Gain Versus Frequency

$$\frac{\Theta_y}{\Theta_\varepsilon} = \frac{G}{HS\left(1 + \frac{S}{\omega_c}\right)\left(\frac{S^2}{\omega_n^2} + \frac{2kS}{H\ \omega_n} + 1\right)} \qquad (12)$$

The stability criteria for this loop becomes:

$$\omega_c < \left(\frac{2k}{H}\right)^{1/2} \omega_n \qquad (13)$$

Comparing equation 13 to equation 11, it is apparent that the maximum crossover frequency has been increased by a ratio of

$$\left(\frac{H}{2k}\right)^{1/2}$$

Using the gyro parameters listed previously the maximum crossover frequency is on the order of 2 rad/sec. This still yields too low a bandwidth for most applications.

Modifying Inherent Nutation Damping of Rotor - **From the standpoint of simplifying the fluidic control loops, the ideal solution to the stability problem would be to** provide the required damping in the rotor mechanism.

The minimum rotor damping requirement for a loop with proportional gain can be estimated from equation 11. Assuming ω_c must be 100 rad/sec, ω_n = 520 rad/sec and H = .025 in.lb.sec. Then:

$$k > \frac{H}{2}\left(\frac{\omega_c}{\omega_n}\right) = 2.4\ (10^{-3})\ \text{in.lb.sec.}$$

A method of obtaining rotor damping is illustrated by the following sketch.

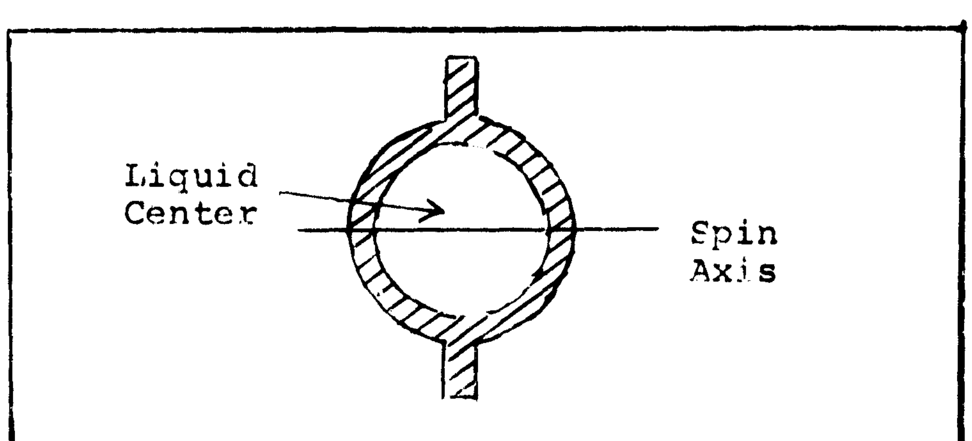

The spherical bearing surface of the rotor is made as a hollow sphere. The sphere is filled with a liquid and sealed. Gyro nutation can be qualitatively described as an oscillation of the rotor about its minor axes. To an observer looking at the rotor along a minor axis, nutation appears as an oscillation of the rotor flange about that axis with a frequency of oscillation equal to rotational frequency multiplied by the ratio of major to minor moments of inertia. The core of the liquid filled rotor tends to hold a space referenced attitude. As the rotor oscillates about a minor axis shear forces will be induced between the rotor shell and the non-oscillating inner core of the liquid. These forces are a function of the component of rotor velocity about a minor axis and will damp nutation.

This technique has been successfully used to provide damping on torsional spring-mass frequency references used in fluidic phase and amplitude discriminator circuits. There is a wide range of fluids that can be used - best results have been obtained with a silicone fluid with a viscosity of 2000 centistokes. Extrapolation of damping factors obtained on the spring-mass references indicates that rotor damping factors of 3 (10^{-3}) in.lb.sec. can be obtained. This approach used in conjunction with lag compensation will give adequate bandwidth.

This approach has several disadvantages:

1. Rotor fabrication is more difficult -- the rotor must be made in two halves and the two halves joined and finish lapped after assembly.

2. It restricts the bearing and rotor design to the type of configuration used in the feasibility model. It cannot be effectively applied to the "inside-out" rotor configuration.

3. Care must be exercised in filling the rotor to insure that no voids are present in the liquid. Voids could cause shifting of the rotor center of gravity.

<u>Parallel Damping Loop</u> - This loop is used in conjunction with the primary torquing loop. The output of the damping loop is applied to a second set of torquing nozzles. This torque is applied about the axis on which the angular displacement occurs.

The open loop transfer function for this approach is derived in the same manner as used to derive the gyro transfer function (equation 7). The torques applied about the x and y axis are given by:

$$T_x = -G\Theta_{\varepsilon y} - gS\Theta_{\varepsilon x}$$

$$T_y = G\Theta_{\varepsilon x} - gS\Theta_{\varepsilon y}$$

Where g is the gain of the derivative circuit used as the damping amplifier. The inherent damping of the bearing (k) is small compared to required damping factors and can be neglected.

The open loop transfer function then becomes:

$$\frac{\Theta_y}{\Theta_\varepsilon} = \frac{G\left(\frac{gIS^3}{G^2} + \frac{g^2S^2}{G^2} + \frac{HS}{G} + 1\right)}{HS\left(\frac{I^2S^3}{GH} + \frac{IgS^2}{GH} + \frac{HS}{G} + 1\right)} \tag{14}$$

The practical values of angular momentum this equation reduces to:

$$\frac{\Theta_y}{\Theta_\varepsilon} \approx \frac{G\left(\frac{gS^2}{G\omega_n} + \frac{g^2\ S}{IG\omega_n} + 1\right)}{HS\left(\frac{S^2}{\omega_n^2} + \frac{gS}{H\omega_n} + 1\right)} \tag{15}$$

It is apparent from the preceding equation that the damping amplifier is damping the pole occurring at the gyro nutation frequency (ω_n) and has added a zero to the transfer function. If the damping amplifier gain (g) is made numerically equal to G/ω_n, thequadratic in the numerator of equation 15 is identical to the guadratic in the denominator and the open loop transfer function reduces to:

$$\frac{\Theta_y}{\Theta_\varepsilon} = \frac{G}{HS} \tag{16}$$

For values of g less than G/ω_n the zero will occur at frequencies higher than the nutation frequency and for values of g greater than G/ω_n the zero will occur at a frequency lower than the gyro nutation frequency.

Figure 8 is an amplitude vs. frequency plot of the transfer function where G/H has been selected to give a 100 rad/sec cross-over and the damping amplifier gain is .8 of the gain required to get exact cancellation of the poles and zeros. It is apparent that nutation damping is marginal and for reliable operation the damping amplifier gain should be a minimum of G/ω_n.

Lead Compensation - The transfer function for the gyro with lead compensation can be derived from equation 5. The proportional gain (G) is replaced by G (1+tS).

The resulting transfer function becomes:

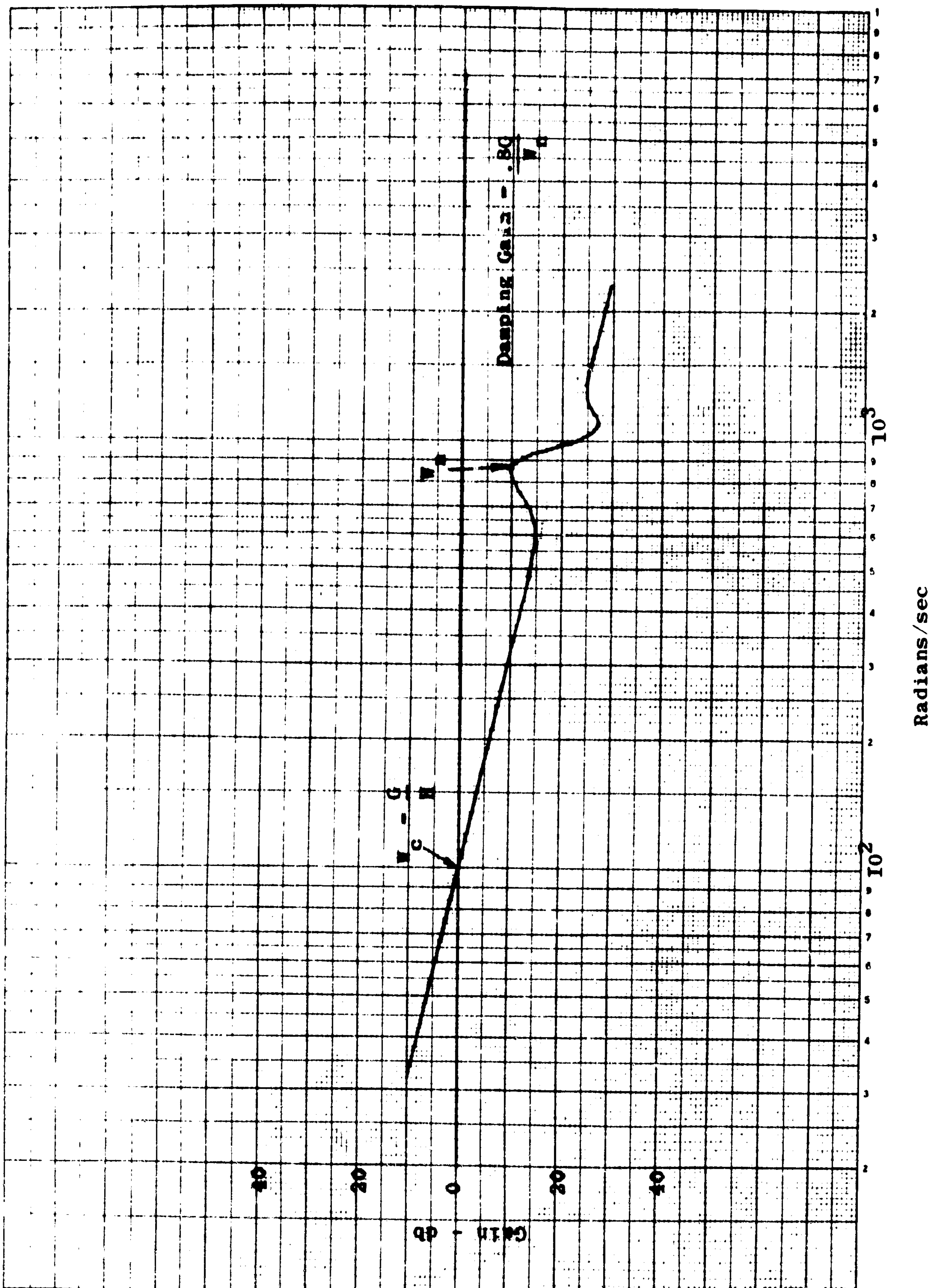

Gain - db
40
20
0
20
40
$W_c = \frac{G}{H}$
W_n
Damping Gain = $\frac{.8G}{W_n}$
10^2
10^3
Radians/sec

$$\frac{\Theta_Y}{\Theta_\varepsilon} = \frac{G\left[\left(\frac{Gt+H}{G}\right) tS^2 + \frac{(2tC+H)S}{G} + 1\right]}{HS\left[\frac{I^2S^3}{GH} + \frac{2kIS^2}{GH} + \frac{(Gt+H)S}{G} + 1\right]} \tag{17}$$

For practical values of angular momentum the transfer function reduces to:

$$\frac{\Theta_Y}{\Theta_\varepsilon} \approx \frac{G\ (2tG+H)}{H\ (Gt+H)S} \frac{\left[\left(\frac{Gt+H}{2Gt+H}\right) tS + 1\right]}{\left[\frac{I^2S^2}{H(H+Gt)} + \frac{2kIS}{H(H+Gt)} + 1\right]} \tag{18}$$

A test for the effectiveness of the compensation network is to let the inherent nutation damping (k) of the rotor approach zero. It is apparent from the preceding transfer function that k is a direct multiple of the damping coefficient of the quadratic and the loop will go unstable as k approaches zero. Lead compensation is then ineffective in damping nutation.

Gyro Design

Design Goals - The following design goals were used as a guide in selecting the gyro gains and the physical parameters of the rotor and air bearing.

- maximum linear range — 15°/sec input about either axis
- threshold — .02°/sec
- bandwidth — 50 to 100 rad/sec
- g capability — 15 g along any axis

Rotor and Air Bearing Design - The physical size of the gyro rotor is determined to a large extent by the maximum range and bandwidth requirements. Past experience on the type of loops required for nutation damping indicated that the nutation frequency should not exceed 500 rad/sec. The bandwidth of the damping amplifiers becomes limiting for higher frequencies. The selected rotor configuration has a nutation frequency equal to 1.7 times the spin frequency, this establishes the rotor spin speed at about 5000 RPM. Using this spin speed the moment of inertia of the rotor about the spin axis is selected to match the maximum torque capability of the gyro torquing loops. Based on these considerations a two inch diameter aluminum flange was selected. The flange is .1 inch thick and is shrunk fit on a .75 inch diameter steel ball.

The hydrostatic air bearing consists of two spherical inner surfaces which surround the rotor sphere. Figure 9 is a cross section of

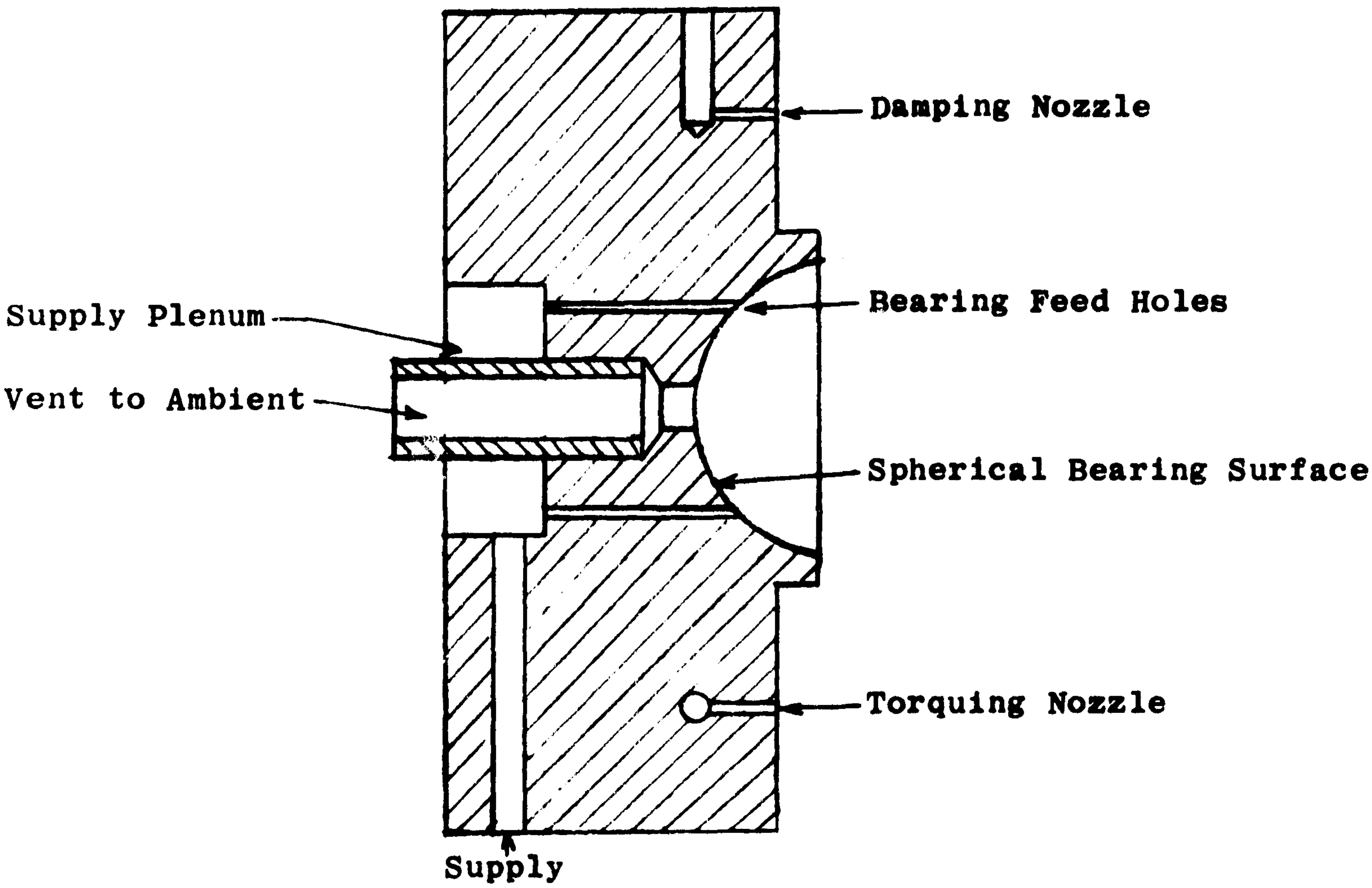

Figure 9. Bearing Cross Section

the aluminum bearing block. The block also contains the torquing nozzles, the supply plenum for the bearing and serves as a mounting surface for the amplifiers. The bearing has eight .02 inch diameter feed holes evenly spaced along a 50° latitude line of the bearing. The pole of the bearing is vented to ambient to permit gas flow from the pole as well as the equatorial region. Bearing tests indicated that both stiffness and dynamic stability were improved by the addition of the polar vent. The bearing surface was fabricated by machining the cavity to rough dimensions. The surface was then coined and lapped to final dimensions.

The pertinent characteristics of the bearing and rotor are given in Table 1.

Table 1

Bearing-Rotor Characteristics

Rotor	
Rotor diameter	2 inches
Rotor weight	.086 lbs.
Moment of inertia about spin axis	4.8 (10^{-5}) in.lb.sec^2
Moment of inertia $\perp$ to spin axis	2.8 (10^{-5}) in.lb.sec^2
Operating speed	5000 RPM
Bearing	
Load capacity	1.5 lbs.
Supply pressure	30 psig
Bearing flow	.005 lb/sec
Nominal gap	.0015 inches
Feed holes (8 per half)	.02 inch diameter

Primary Torquing Loop and Angle Pickoff - The area of the torquing nozzles and the output stage nozzle is determined by the maximum input rates applied to the gyro. The required torque is given by:

$$T = H\omega_{max}$$

The angular momentum of the rotor is .025 in.lb.sec when spinning at 5000 RPM and the max input rate is 15°/sec. The required torque is then .0065 in.lb. The torquing nozzles have a moment arm of .875"; hence, the required nozzle force is .0075 lb.

The size of the torquing nozzle and amplifier jet nozzle can be obtained from Figure 10. Figure 10 is a plot of measured differential force from a nozzle being supplied from a fluidic amplifier stage of various supply pressures. The highest ratio of force to supply pressure is obtained when the torquing nozzle area is equal to the area of the driving amplifier.

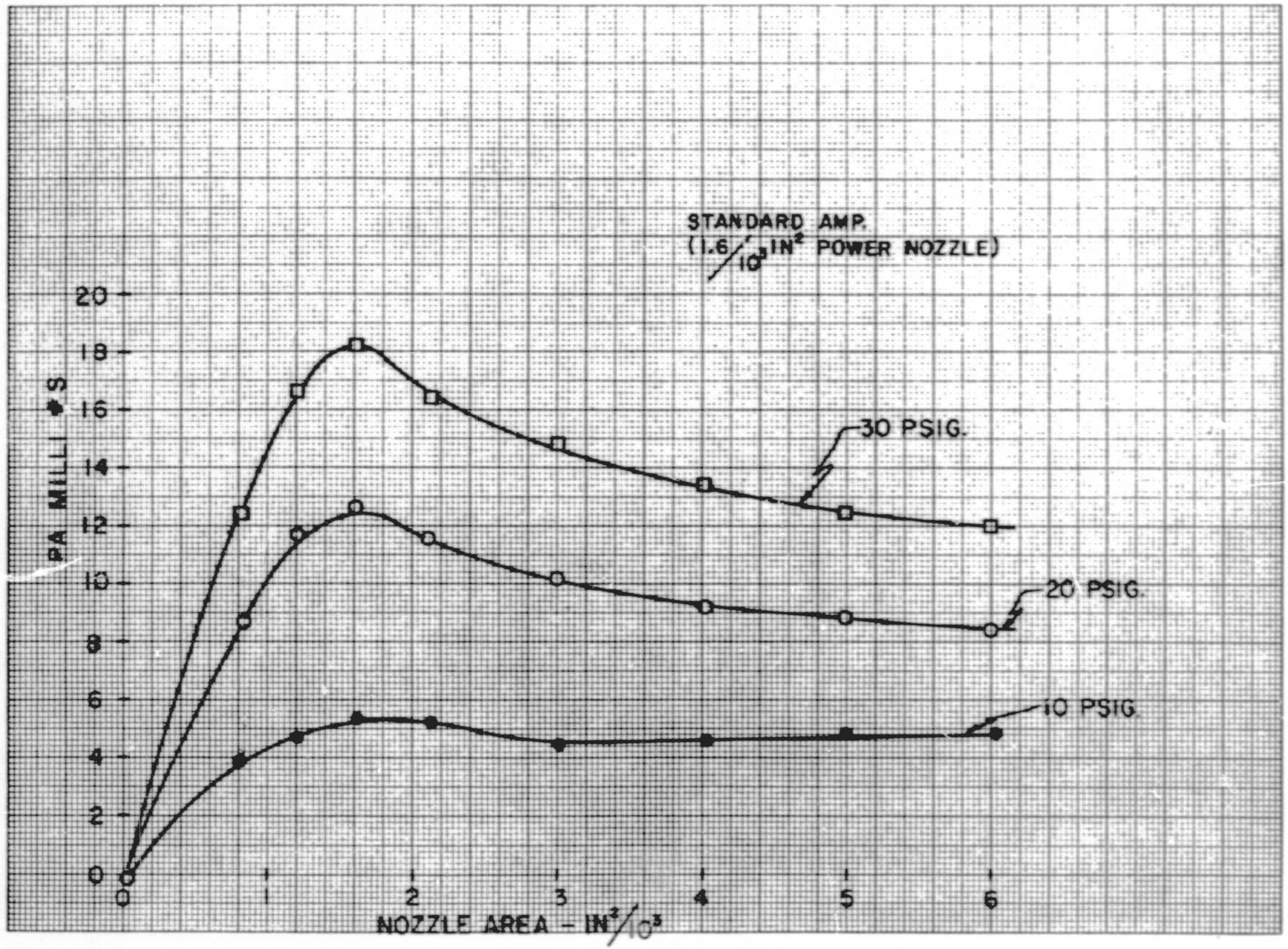

Figure 10. Force Versus Nozzle Area

An $8/10^4$ in^2 amplifier operating at a 30 psig supply will give a force output of .009 lbs which is more than adequate. This area is equivalent to a standard element with an aspect ratio of 2.0. The output torquing nozzle area is made equal to the amplifier nozzle area.

A schematic of the angle pickoff is shown in Figure 11. The sensor is a bridge circuit with two fixed and two variable resistors. The variable resistors are two .02 inch diameter nozzles directed at the edges of the rotor flange. Angular displacement of the rotor flange relative to the pickoff results in a decrease of effective area on one orifice and an increase on the other.

The output of the sensor as a function of angular displacement is shown in Figure 12. A standard General Electric proportional amplifier was used as a load on the sensor output. The sensor has a range of .01 radians and a gain of 30 psi/radian.

The overall gain of the torquing loop is established by the gyro bandwidth requirements. The required gain is equal to the product of angular momentum and bandwidth. Using a 100 rad/sec bandwidth as a design goal and an angular momentum of .025 in.lb.sec, the required gain is 2.5 in.lb/rad. Factoring in the torquing nozzle area and moment arm the overall gain becomes 3600 $lb/in^2/rad$. The sensor gain is 30 $lb/in^2/rad$; hence, an additional gain of 120 is required. The additional gain is provided by three standard amplifiers (.02" nozzle width) with aspect ratios of .8, 1.6 and 2.0.

<u>Damping Amplifier</u> - Equation 15 defined the damping amplifier gain requirements. The gain must be equal to the primary torquing loop gain divided by nutation frequency. The torquing loop gain has been established at 2.5 in.lb/rad and the nutation frequency at 140 Hz (880 rad/sec); hence, the damping amplifier gain (g) must equal .003 in.lb.sec.

The input to the damping amplifier will be a signal proportional to angle; a derivative network is incorporated in the damping loop to obtain the damping coefficient.

The output of the damping loop is applied as a torque about the sensitive axis of the associated channel. Any steady state gain in the damping amplifier will result in a torque to precess the gyro rotor about the sensitive axis associated with the second channel. This precession is interpreted as an input rate and the second channel generates an equal and opposite torque. Steady state gain in the damping loop then introduces cross coupling and erroneous outputs and must be minimized. This becomes a prime consideration in the selection of the damping amplifier configuration.

The derivative network selected consists of two fluidic inductors shunting the output amplifier to local ambient. The steady state gain is reduced to acceptable levels by making the inherent resistor of the inductor much smaller than the amplifier output

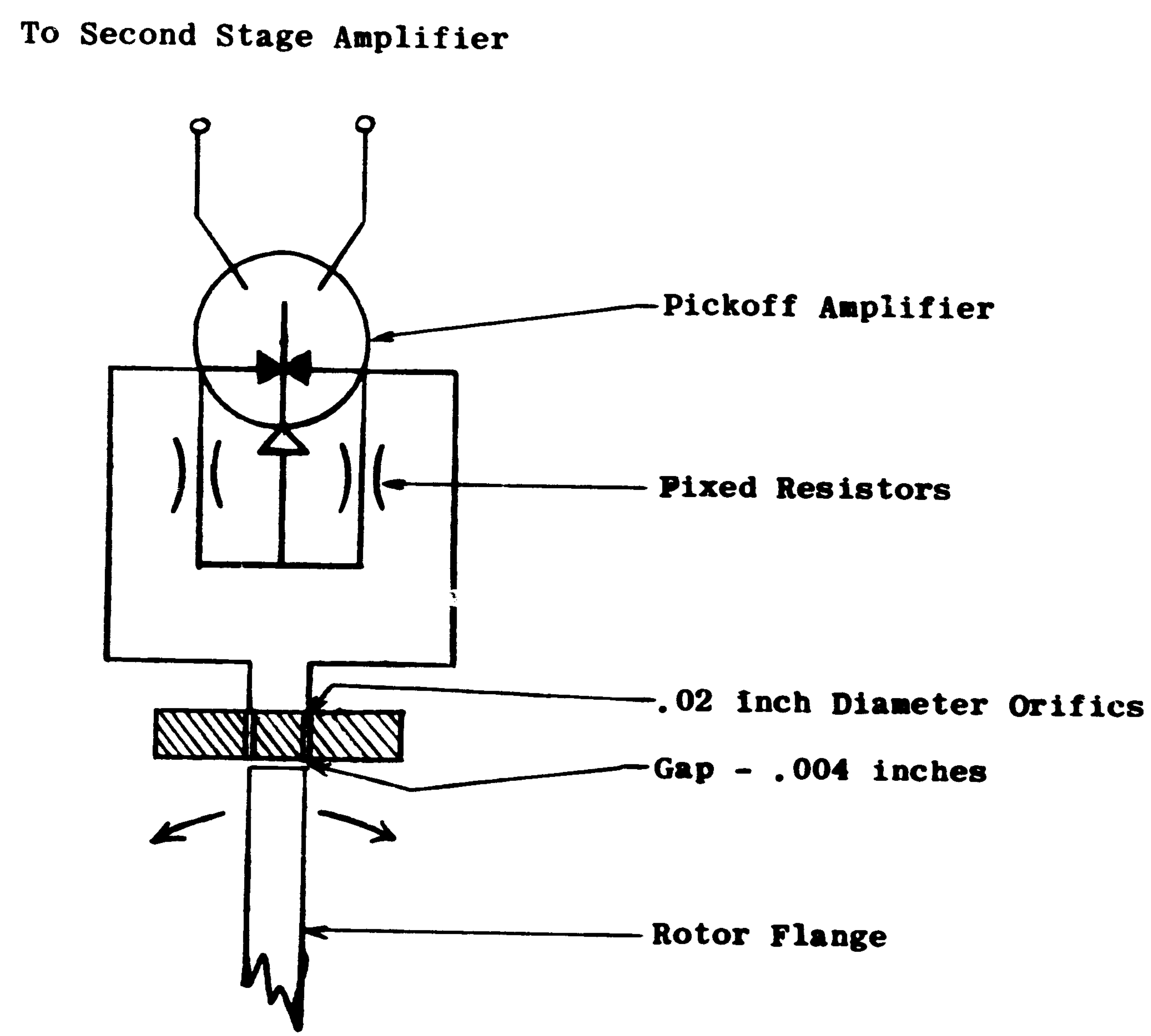

Figure 11. Angle Pickoff Schematic

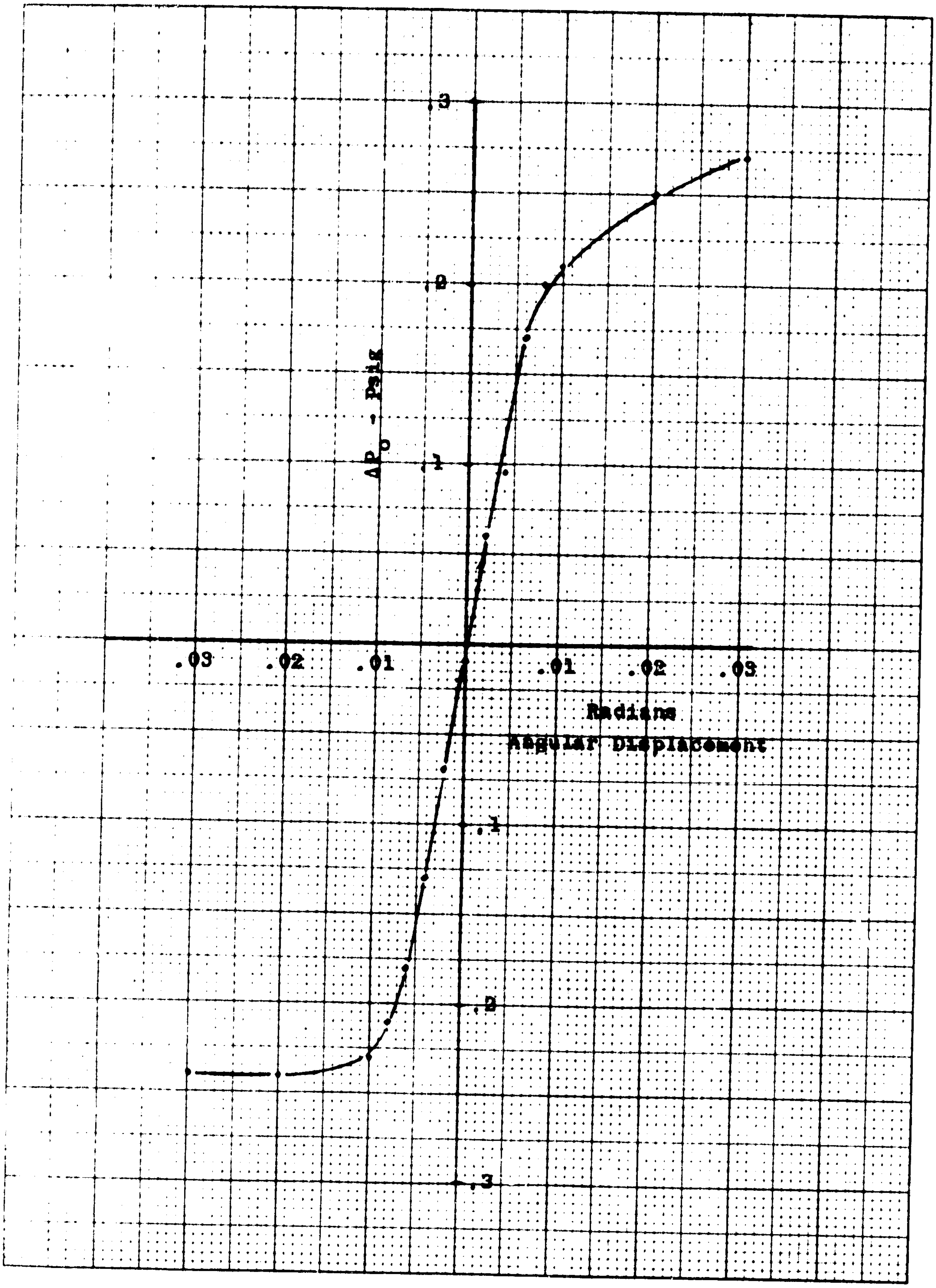

Figure 12. Angle Pickoff Characteristic

resistance.

The output characteristics of this type of a network is shown in Figures 13 and 14. An inductor length in the range of 12 to 6 inches will give adequate phase lead at the nutation frequency of 140 Hz. A 12 inch length was selected because of the higher gain at the nutation frequency. With a $8/10^4$ in^2 damping nozzle and a .875" moment arm, the overall gain required to satisfy a .003 in.lb.sec damping coefficient is 4.3 $lb.sec/in^2$. The combined gain of the angle pickoff and the damping amplifier is $3/10^2$ $lb.sec/in^2$; hence, an additional gain of 140 is required. The damping amplifier utilizes the angle pickoff and the first two stages of the primary torquing loop; one additional stage is required to satisfy the overall gain requirement.

Testing

The primary test effort on the gyro was directed at identification of the extraneous torques acting on the gyro rotor, verification of fluid amplifier gains in the assembled package and demonstration of overall stable operation. The extraneous torques acting on the gyro rotor were of such magnitude that quantitative measurements of gyro scale factor, threshold and bandwidth were difficult to obtain.

Torquing and Damping Loop Gain - The purpose of these tests was to measure the overall gain of the loops as assembled on the gyro. Figure 15 is a plot of the differential pressure across the torquing nozzles as a function of angular displacement of the rotor flange. The overall gain is 1500 psi/rad or about 40% of the gain obtained on the same circuit using a simulated angle sensor as the input. The gain reduction is attributable to the fact that the angle sensors had to be displaced "off center" to conform to the zero torque axis of the bearing. This caused the rotor flange to be canted relative to the pickoff when at the nulled position. At the reduced gain the gyro bandwidth is estimated to be 40 rad/sec.

The static gain of the damping loops was determined by measuring the pressure differential across the damping nozzles as a function of angular displacement of the rotor. The results are shown in Figure 16. The measured static gain is 35 psi/rad. Comparing this to the primary torquing loop gain of 1500 psi/rad a cross coupling of 2.3% will result. The damping coefficient was measured by reducing the operating speed of the gyro to a value which made the loop oscillate at the nutation frequency. The output of the damping loop was then compared to the output of the primary torquing loop. This instability occurs at a nutation frequency of 500 rad/sec. The measured damping coefficient is 2 $lb.sec/in^2$ or 45% of the damping coefficient required for a 100 rad/sec bandwidth. The decreased angle sensor gain is the primary contributor to the decreased damping coefficient. The damping coefficient has decreased by the same ratio as the primary torquing loop and

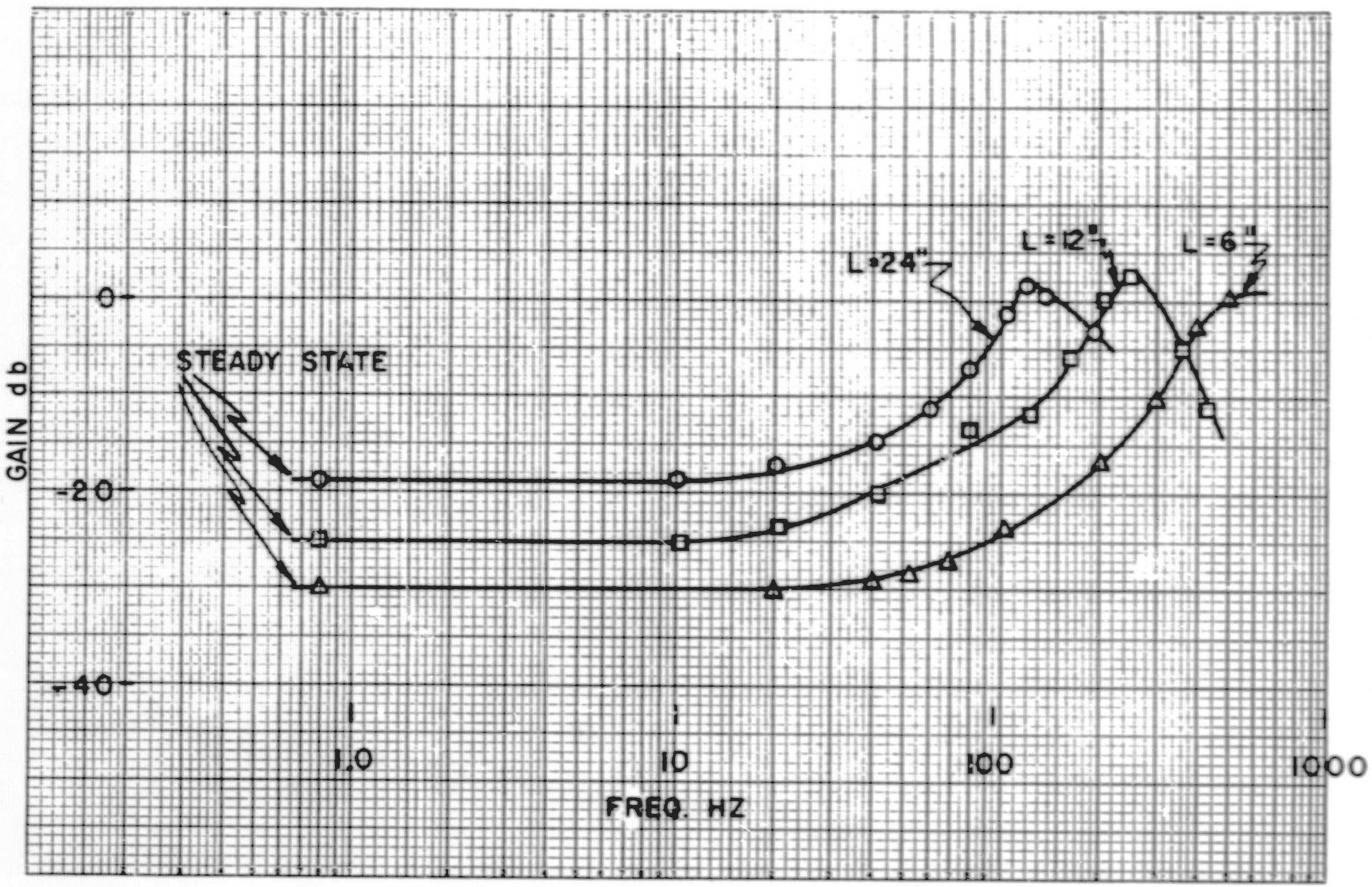

Figure 13. Derivative Circuit - Amplitude

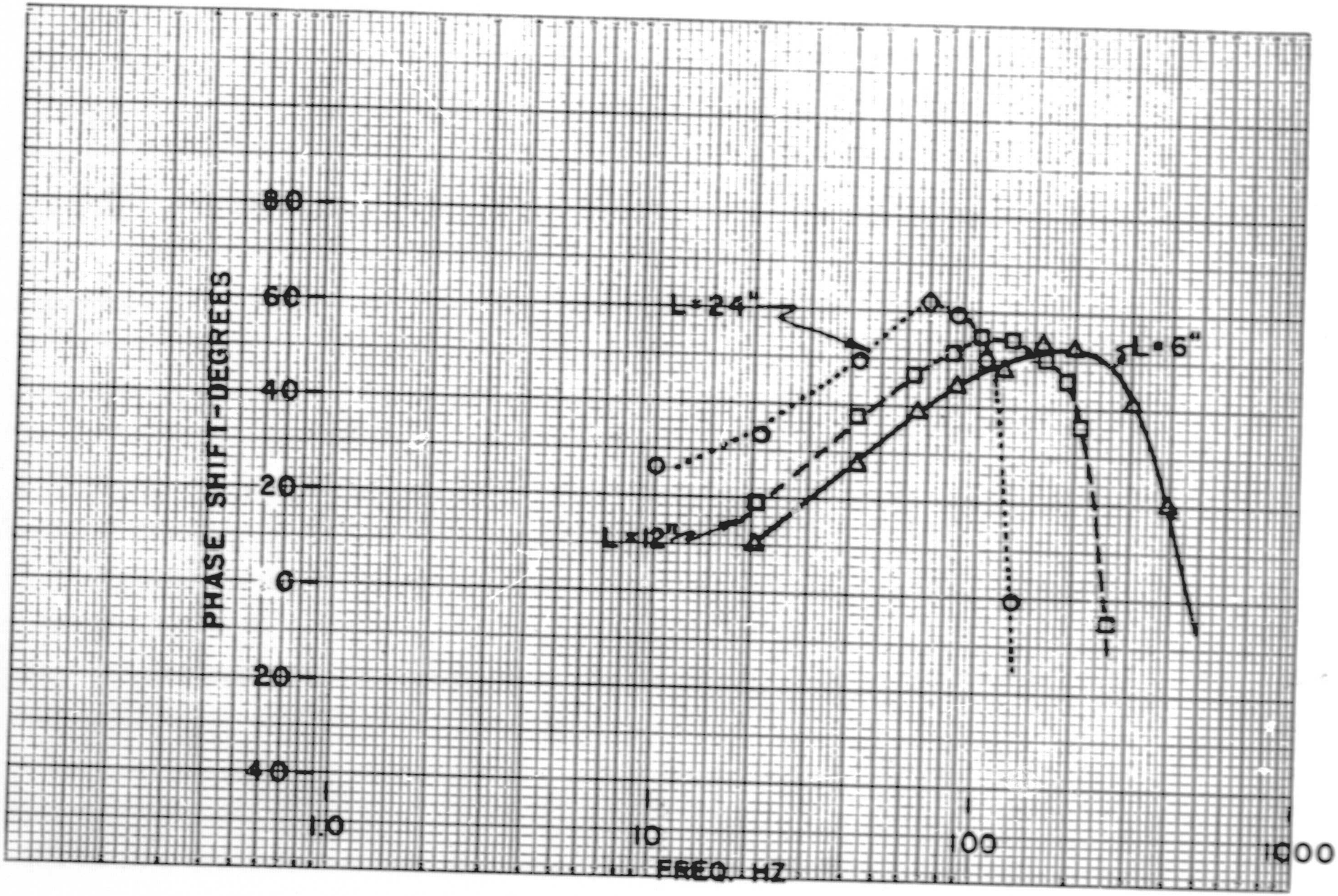

Figure 14. Derivative Circuit - Phase

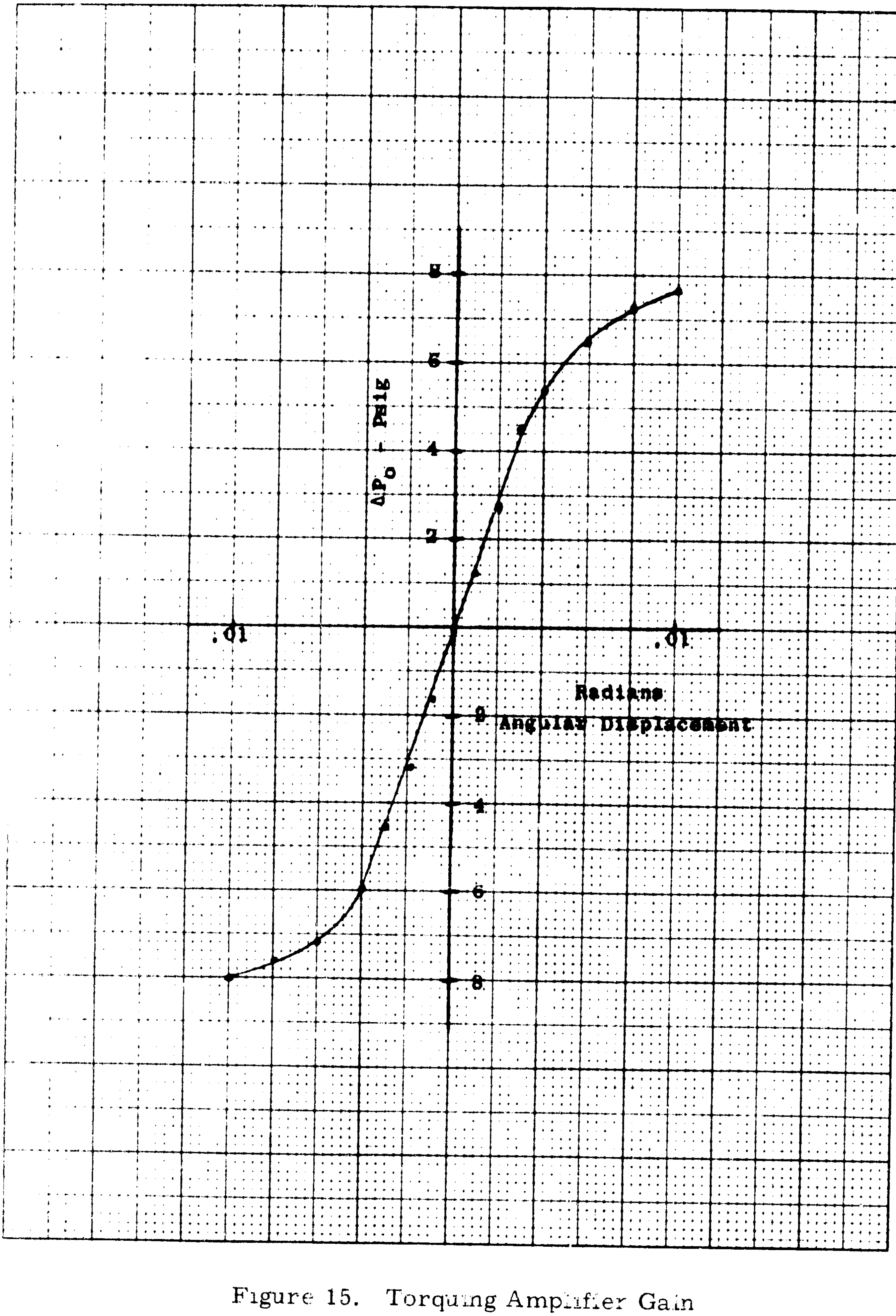

Figure 15. Torquing Amplifier Gain

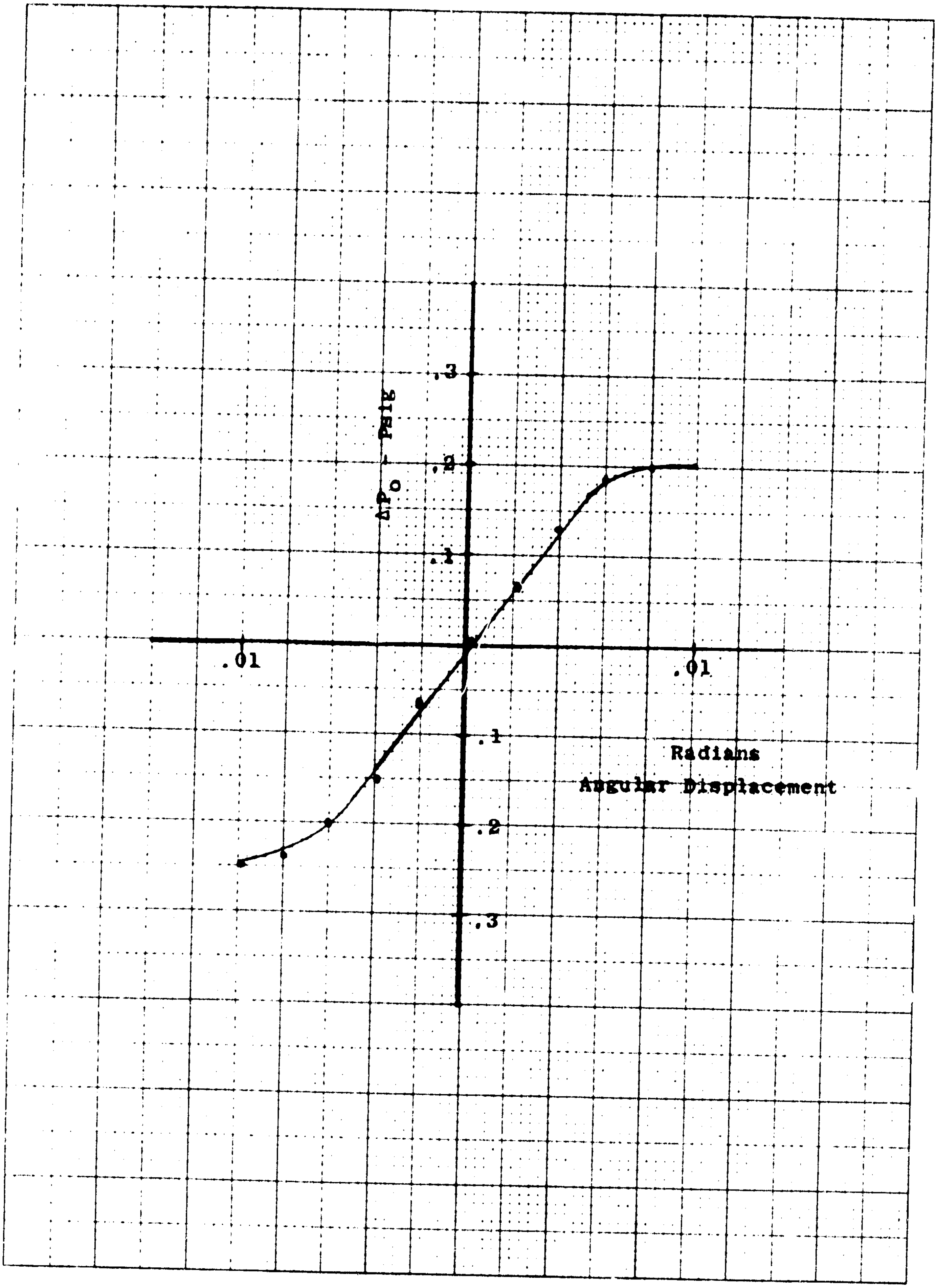

Figure 16. Static Gain of Damping Loop

there is adequate damping in the loop for a 40 rad/sec bandwidth.

Air Bearing Tests - A series of tests were conducted to obtain a quantitive measurement of the torques acting on the gyro rotor. These tests were open loop tests where the precession pattern of the rotor was observed. The gyro torques on this configuration can be catagorized as follows.

1. Torques which are independent of the orientation of the gyro spin axis relative to the bearing structure.
2. A torque gradient about the same axis as the rotor spin axis is displaced.
3. A torque gradient about an axis perpendicular to the axis on which rotor displacement occurs.

The torques which are independent of the orientation of the spin axis impart a steady state precession to the gyro rotor, in the absence of any other sources of torque the spin axis will precess at a constant rate until a physical limit is encountered. If a second torque source (with the characteristics of a torque gradient) exists, then the gyro spin axiswill seek an orientation where the summation of torques is equal to zero. If the torque gradient is known, then the magnitude of the bias torque can be deduced by observing the angular displacement of the spin axis relative to the axis of symmetry of the bearing pad.

Torque gradients occurring about the same axis as the rotor is displaced cause a low frequency oscillation of the spin axis relative to the bearing structure. The torque gradient is equal to the angular momentum of the rotor multiplied by the frequency of oscillation in rad/sec. Observation of the period for a known angular momentum is then a convenient and accurate measure of the torque gradient.

Torque gradients which occur about an axis perpendicular to the axis of displacement will generally cause the rotor spin axis to be slaved to the bearing in a non-oscillatory mode. The magnitude of this gradient can be deduced by applying a step input of displacement to the case and observing the settling time of the rotor spin axis. The magnitude of the torque gradient is given by the angular momentum divided by the settling time.

By observing the precession pattern of the rotor under a number of different test conditions the major contributors to the extraneous torques could be identified. For example, the torques associated with the bearing pad were measured with the rotor in a free coasting mode. These torques were then compared to the torques acting on the rotor when speed was maintained by the spin jets. In a like manner, the contribution of the angle pickoffs and primary torquing nozzles were determined. The contribution of the torquing nozzles was measured with equal bias pressures applied to all four nozzles and is a measure of cross coupling through the two torquing loops.

The results of these tests are listed in Table 2. T_B designates a bias torque; T_g, a torque gradient about the axis of displacement and $t_{g\perp}$, a torque gradient about the axis perpendicular to axis of displacement.

Table 2

Rotor Torques

Torque Source	T_B	T_g	$T_{g\perp}$
Air Bearings			
10 psig supply	.001 in #	.024 in #/rad	
30 psig supply	.0015 in #	.04 in #/rad	
Spin Jets			.25 in #/rad
Angle Pickoff		.02 in #/rad	
Torque Jets (5 psig)	.0001 in #	.05 in #/rad	

These torques can be transcribed into equivalent drift rates or cross coupling ratios on the gyro.

The air bearing bias torque at 30 psig is equivalent to a gyro drift rate of 3.5°/sec. This torque resulting from bearing misalignment will be g sensitive and thus cannot be readily compensated. An "inside-out" rotor configuration where assembly misalignment occurs on the rotating rotor will essentially eliminate this component. The air bearing also contributes a torque gradient which introduces cross coupling. With a 30 psig supply on the bearing, the cross coupling will be 4%, if the primary torquing loop gain is set to establish a 40 rad/sec gyro bandwidth.

The torque gradient from the spin up jets will influence the gyro scale factor. With the primary torquing loop set for a 40 rad/sec bandwidth the measured torque gradient will cause a 25% reduction in scale factor.

The torque gradient from the angle pickoffs and the torque jets introduce cross coupling in the same manner as the bearing torque gradient. The torque gradient from the various sources are additive so the total torque gradient causing cross coupling is .29 in.lb/rad. This is equivalent to 30% cross coupling on a 40 rad/sec bandwidth gyro.